PHYSICAL REVIEW B VOLUME 52, NUMBER 7 15 AUGUST 1995-I

Molecular-dynamics simulations of nickel oxide surfaces

P. M. Oliver,* G. W. Watson,† and S. C. Parker‡
School of Chemistry, University of Bath, Claverton Down, Bath BA2 7AY, United Kingdom

(Received 16 March 1995)

Molecular-dynamics-simulation techniques have been used to investigate the effect of temperature on the three low index surfaces of nickel oxide. The surface energies for the {100}, {110}, and Ni {111} surfaces have been calculated as a function of temperature for NiO. The surface energies for all three surfaces were essentially constant up to 2000 K, when surface melting was observed for the less densely packed surfaces such as the {110} and Ni {111} surfaces. The {110} surface reconstructed to give {100} microfacets that are densely packed, and hence the surface disorder was less than the Ni {111} surface. The defective (Ni^{3+}) Ni {111} surface showed a similar tendency but was less marked, partly due to the increased charge at the surface. The oxidation energy was negative, indicating that thermodynamically the surface would oxidize.

I. INTRODUCTION

An understanding of the factors controlling the structure and the stability of solid interfaces at the atomic level is important for developing systematic ways of modifying and ultimately controlling surface behavior. Atomistic simulation represents a useful tool for predicting and rationalizing the properties of oxide interfaces.[1-3] These include the study of disordering and surface premelting of the low index faces of copper[4] and diffusion pathways in grain boundaries of NiO.[5] More recently, this methodology has been applied to understanding the effect of habit modifying ions such as Li^+ and Mg^{2+} on the growth and morphology of $CaCO_3$. The calculated morphologies were shown to give good agreement with experiment.[6] However, much of the previous work on oxide surfaces has not treated the effect of temperature. Two notable exceptions include the work of Masri and Tasker,[7] where they used the harmonic approximation within lattice dynamics to model calcium-doped MgO. This treatment of temperature is limited because the harmonic approximation cannot model thermal expansion (extrinsic anharmonicity) and breaks down at high temperatures due to intrinsic anharmonic effects.[8] The second study used the molecular-dynamics simulations of Ferneyhough *et al.*,[9] where they compare the melting point of thin {100} slabs of MgO using rigid-ion and shell models.

In this paper we have considered NiO, which has the same simple cubic structure as MgO with sixfold coordinated Ni^{2+} and O^{2-}. However, while pure MgO reflects the underlying lattice in its morphology by forming cubic crystallites, NiO does not. Experimentally, NiO is shown to express {111} faces in the morphology either in the form of a cuboctahedron[10] or an octahedron.[11] On the basis of static simulations[12] on NiO we have postulated that the {111} surface is stabilized by oxidation. However, this neglected explicit treatment of temperature. The observed morphologies were the result of annealing for 55 h at 1800 K.[10] Therefore, we present the results of molecular-dynamics (MD) simulations on the low index stoichiometric {100}, {110}, and {111} surfaces of NiO and the most stable defective surface, as identified by Oliver and co-workers,[12] the oxidized Ni {111} surface. In addition, work on metal surfaces at high temperatures[4] has suggested the intriguing premelting phenomena that has not been observed for oxides.[9] We have therefore considered temperatures up to the bulk melting point for NiO.

II. METHODOLOGY

All of the molecular-dynamics simulations presented in this paper use the MD code QCTPMD.[13,14] This employs the constant-pressure algorithm of Parrinello and Rahman[15] and the Nose-Hoover[16,17] constant-temperature algorithm. The constant-pressure method allows a dynamical change in both the lattice vectors and angles with time. The constant-temperature method effectively places the cell in contact with a heat bath. Energy is allowed to transfer between the simulation box and the heat bath, keeping the simulation box within the constant-temperature ensemble. The ensemble used for the bulk calculations is therefore the isobaric, isothermal ensemble (*NPT*). Bulk simulations of NiO were performed using a cell containing 512 ions periodic in three dimensions. Initial random velocities were assigned and scaled for 2.5 ps (2 500 time steps) using the *NPE* ensemble, and then a further 2.5 ps using the *NPT* ensemble before the main data-collecting run of 10 ps using the *NPT* ensemble. This gave the unit-cell dimensions as a function of temperature. The surfaces were simulated by forming slabs comprised of planes of ions perpendicular to the surface. The {100} and {110} surfaces presented no problems, as they are formed on cleavage into layers of stoichiometric NiO. the {111} surface, in contrast, requires further consideration. Unlike complementary studies on metal surfaces, the electrostatics need to be taken into account. There are three types of surfaces as identified by Tasker:[18] types I, II, and III. In type-I surfaces the stacking plane is neutral, being composed of both cations and anions in a stoichiometric ratio resulting in no dipole perpendicular to the surface. Type-II surfaces contain a series of charged planes, making a symmetric repeat unit that has no net dipole perpendicular to the surface. Type-III surfaces are composed of alternately charged planes, producing a dipole perpendicular to the surface if cleaved between the planes. The Coulombic sum for such a surface cannot be evaluated as it is divergent.[19] If such surfaces are to be studied, then a reconstruction will have to be made to the surface such that the dipole is cancelled. In this study both the {100} and {110} of NiO are type-I surfaces and therefore require no reconstruction. However, the {111} surface is type III and must be reconstructed, the simplest method of which is to make the surface layer 50% vacant by transferring 50% of the ions to the bottom of the repeat unit, thus canceling the dipole. Two surfaces can be formed, the Ni {111} and the O {111}. In this study only the Ni {111} is investigated as the oxidized Ni {111} was identified as the most stable by Oliver and co-workers,[12] involving the formation of Ni^{2+} vacancies and compensating holes. This is discussed in more detail in Sec. V.

The properties of the {100}, {110}, Ni {111}, and oxidized Ni {111} surfaces were then evaluated within the canonical ensemble (*NVT*) by constraining the lattice constant to be that determined from the bulk calculation, i.e., constant area for the surface simulation. The slab energy of the NiO surfaces {100}, {110}, Ni {111}, and oxidized Ni {111} were calculated using a slab of sizes 640, 896, 1280, and 1216 ions, giving rise to slab depths 20 Å (10 layers), 22 Å (14 layers), 25 Å (21 layers), and 22 Å (19 layers), respectively, to ensure convergence of the lattice energy. The slab is periodic in three dimensions with a void of approximately 80 Å between the periodic images perpendicular to the surface.

The forces acting on the ions are described by the Born model of solids. The ions were assigned their formal valence charges with a Buckingham potential to model the short-range interaction between neighboring ions:

$$F_i = \sum_j^{\text{crystal}} \left[-\frac{q_i q_j}{r_{ij}^2} - \frac{A_{ij}}{\rho_{ij}} \exp\left[-\frac{r_{ij}}{\rho_{ij}} \right] + \frac{6C_{ij}}{r_{ij}^7} \right] ,$$

where F_i is the force on ion i, q_i, and q_j are the charges of ions i and j separated by a distance r_{ij}, and A_{ij}, ρ_{ij}, and C_{ij} are potential parameters for interaction i-j.

The potential model selected for NiO was developed by Sangster and Stoneham.[20] The original model included electronic polarizability via the shell model, although most molecular-dynamics codes, including ours, use the rigid-ion model. Work by Gillan[21] has shown that the model needs to be adjusted to reproduce the dielectric constant on removal of the shell-model parameters. This is necessary because the static dielectric constant is important for both defect-formation energies[1] and surface properties.[22] The potential parameters were adjusted and are given in Table I(a). The properties calculated by this new potential using a short-range potential cutoff of 7.0 Å are given in Table I(b), and show adequate reproduction of the experimental properties.

Polarizability can be introduced into MD via the shell model using either the adiabatic approach[27] or conjugate gradient minimization of the shells between each MD step.[28] However, recent calculations[9,29] suggest that there are no significant differences between shell MD and rigid-ion MD for MgO, giving us confidence in the rigid-ion MD technique used in this study.

III. MODELING BULK NiO

The variations in the calculated lattice parameters are given in Fig. 1. From this it is clear that the bulk crystal has melted at 3400 K because the lattice constant is vastly different from the rest of the series. The thermal coefficient of expansion of 3.5×10^{-5} K^{-1} at 1000 K compares well to the experimental value of 3.8×10^{-5} K^{-1} at 1000 K.[30] Thus the potential is able to model the

TABLE I. (a) Fitted potential parameters and (b) comparison of the properties calculated using the fitted and original potential with experiment for NiO.

Interaction	(a) A (eV)	ρ (Å)	C (eV Å^6)
$Ni^{2+/3+}$-O^{2-}	775.0	0.3250	0
O^{2-}-O^{2-}	22 764.3	0.1490	20.37
	(b)		
Property	Original[a]	NiO Fitted	Expt.
Static dielectric constant	12.72	12.78	12.7[b]
High-frequency dielectric constant	5.65	1	5.7[c]
Elastic constants (GPa)			
C_{11}	445	291	270[d]
C_{12}	168	175	105[d]
C_{44}	168	175	125[d]
Lattice parameter (Å)	4.17	4.18	4.17[e]

[a] Reference 20.
[b] Reference 23.
[c] Reference 24.
[d] Reference 25.
[e] Reference 26.

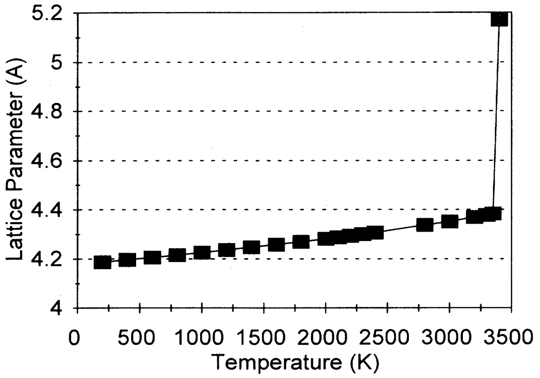

FIG. 1. Calculated lattice parameter as a function of temperature for NiO.

thermal expansion, and hence the bulk structure of NiO as a function of temperature. One possible weakness is that the calculated melting point of approximately 3400 K is well above the experimental temperature of 2257 K. The bulk melting point is the subject of considerable debate.[9,14] This difference may be a result of one or a combination of four factors. The first is the absence of surfaces. This will inhibit melting because of the imposition of three-dimensional periodicity.[9] This will be investigated in Sec. IV. The second is the lack of electronic polarizability, which is known to increase defect energies and may destabilize the melt relative to the bulk, leading to an elevated melting point.[14] We have attempted to minimize this effect by refitting the potential such that the static dielectric constant is in good agreement with experiment. The third factor is too few ions in the simulation cell, which can lead to an imposed order on the system. For the surface slabs discussed in Sec. IV we have used a large number of ions but are restricted due to the CPU time needed. For example, the 1280-ion Ni {111} slab for 30 000 time steps took 100 000 sec on a Convex C3860 single processor. The final factor may be due to the inadequacies in the potential model, but given the agreement between the calculated bulk properties and experimental data,[20] this model is the best that is available.

IV. MODELING OF PURE NiO SURFACES

Molecular-dynamics simulations were performed on the stoichiometric {100}, {110}, and Ni {111} surfaces of NiO. The surface energy as a function of temperature is given in Fig. 2. The surface energy is the energy required to cleave the crystal into two free surfaces. It is calculated from the difference between the surface-slab simulation and the same number of bulk ions per unit area. The surface energy of the {100} surface increases with temperature very slowly, while the {110} and {111} surface energies decrease with increasing temperature up to about 2000 K. Above 2000 K the surface energies of the {110} and {111} surfaces increase rapidly. Above 600 K the {110} surface undergoes a major reconstruction. The surface reconstructs from the initial flat topology to that of a microfaceted topology comprised of {100} facets. This is clearly seen in the average atomic positions at 2000 K (Fig. 3). This is in agreement with a recent static-simulation study of microfacet formation on the {110} surface of MgO (Ref. 31) where the nonfaceted surface had a surface energy of 3.0 J m^{-2}, compared with 2.1 J m^{-2} for the faceted surface. A similar microfaceting effect has been calculated for the {100} surface of TiO$_2$ rutile with {110} microfacets[32] with a faceted surface energy of 2.3 J m^{-2} and a nonfaceted surface energy of 2.1 J m^{-2}.

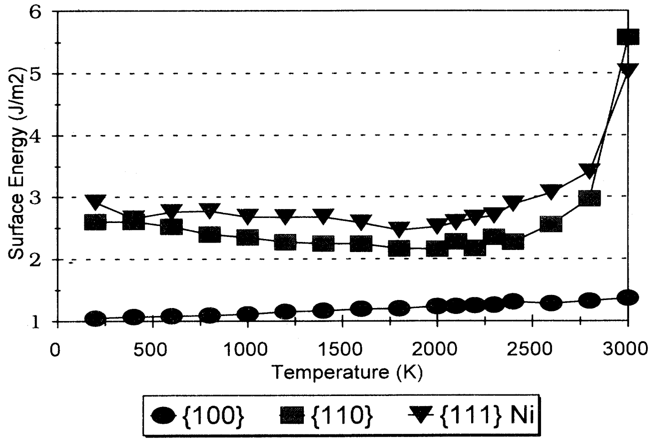

FIG. 2. Surface energy as a function of temperature for the {100}, {110}, and Ni {111} surfaces of NiO.

The approximate melting points of the {100}, {110}, and {111} surfaces are 3400, 3000, and 2800 K, respectively, in comparison to a calculated bulk melting point of 3400 K. All of these melting temperatures are above the experimental temperature of 2257 K. The decrease in melting point for surfaces as compared to the bulk has been calculated previously for the {100} surface of MgO (Ref. 9) using thin slabs four layers thick. The melting point of the {100} MgO surface was identified as approximately 800 K below the bulk. However, the trend observed in this paper indicates that different surfaces melt at different temperatures, with the less densely packed

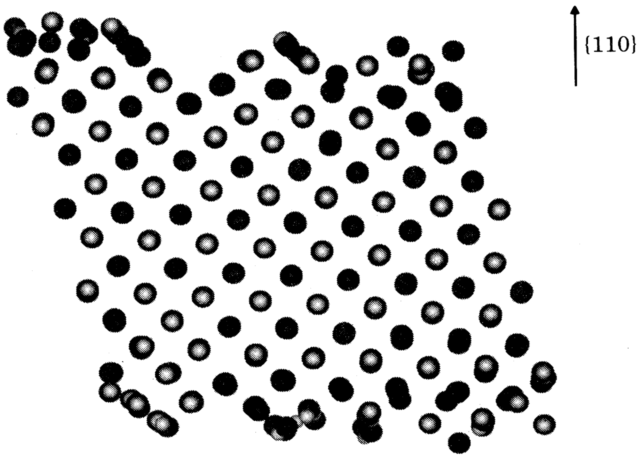

FIG. 3. Average coordinate positions at 2000 K for the {110} surface of NiO [Ni^{2+} (gray) and O^{2-} (black)].

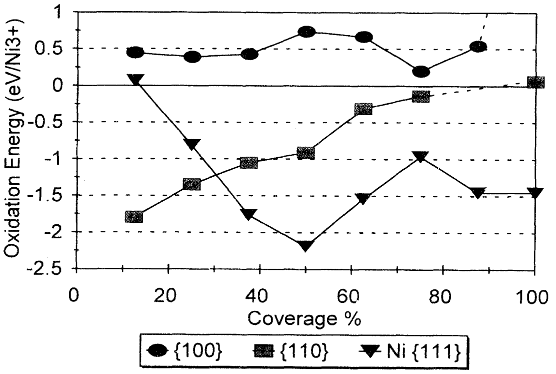

FIG. 4. Oxidation energy as a function of Ni^{3+} hole coverage for the {100}, {110}, and Ni {111} surfaces of NiO.

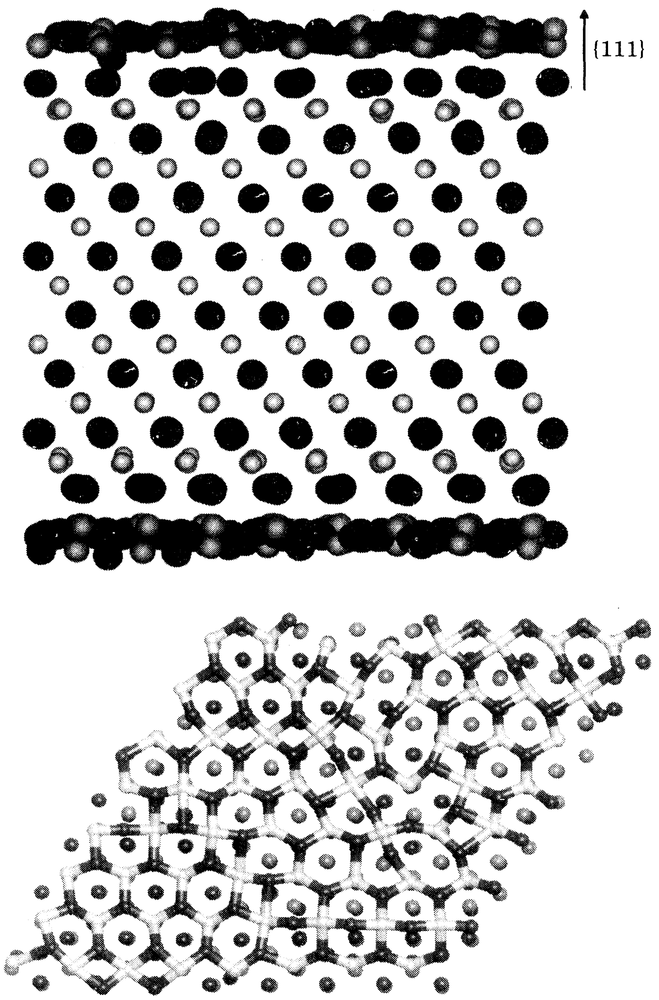

FIG. 5. Average coordinate positions at 2000 K for the oxidized Ni {111} surface showing (a) side view and (b) plan view with surface order emphasized with tubular bonds [Ni^{2+} (gray), Ni^{3+} (large gray), and O^{2-} (black)].

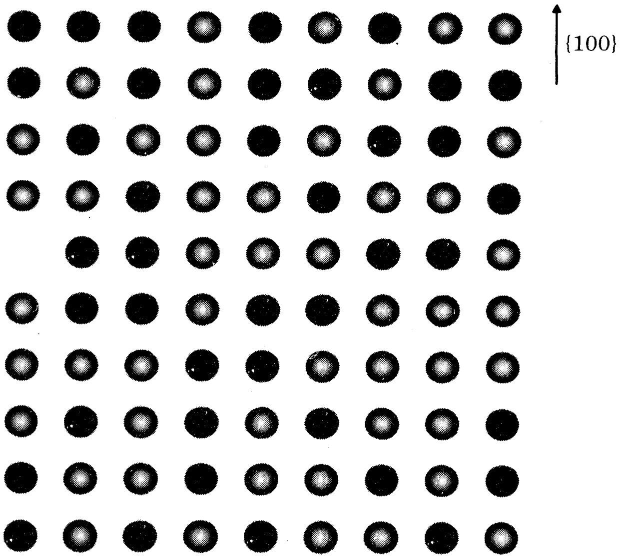

FIG. 6. Average coordinate positions at 2000 K for the {100} surface of NiO [Ni^{2+} (gray) and O^{2-} (black)].

surfaces melting first. The {100} surface was chosen by Ferenyhough *et al.*[9] because it dominates the experimental morphology of MgO. This does not mean that the surface is atomically flat.[33] The surface will be composed of many steps and ridges which could be sites where melting could start, and which should be the focus of future simulations on the melting of MgO.

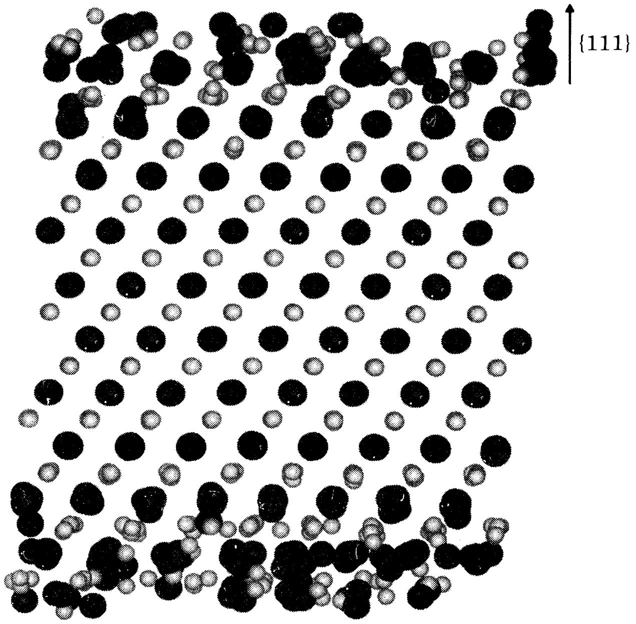

FIG. 7. Average coordinate positions at 2000 K for the Ni {111} surface of NiO [Ni^{2+} (gray) and O^{2-} (black)].

V. OXIDATION OF THE {100}, {110}, AND Ni {111} SURFACES

NiO is oxidized by the following reaction:

$$\mathrm{Ni_{Ni}}+\tfrac{1}{2}\mathrm{O_2}\rightarrow V''_{\mathrm{Ni}}+2h^{\cdot}+\mathrm{NiO}\ ,$$

which involves the formation Ni^{2+} vacancies compensated by holes. The oxidation energy as a function of hole coverage was calculated for the {100}, {110}, and {111} surfaces using the static-simulation methodology as outlined by Oliver and co-workers.[12] The oxidation energy as a function of hole coverage is given in Fig. 4. A negative oxidation energy indicates a favorable exothermic process. The process is not favorable for the {100} surfaces, as the oxidation energies are positive throughout the range of coverages used. For the {110} surface the process is favorable for all coverages with a minimum of -1.7 eV/Ni^{3+} at 12.5% coverage, but becomes less favorable as the coverage is increased. For the Ni {111} surfaces the process is highly favorable with the minimum oxidation energy of -2.2 eV/Ni^{3+} at 50% coverage, and up to 100% coverage the oxidation energy is still exothermic at -1.4 eV/Ni^{3+}. This suggests that for all but low oxygen partial pressures the surface will be fully oxidized. Molecular-dynamics simulations were therefore performed on the 100%-oxidized Ni {111} surface. The initial surface structure of the oxidized Ni {111} for the MD simulation is terminated with a distinct O^{2-} layer followed by a totally oxidized layer of Ni^{3+} and then a layer of O^{2-}. From the average atomic coordinates at 2000 K [Fig. 5(a)] it can be seen that the first two layers have merged, forming a more densely packed surface region. The surface structure is shown in Fig. 5(b), and is comprised of five- and six-membered rings. The oxidation energy for this surface is similar, -1.6 as compared to -1.4 eV/Ni^{3+} for the static simulations, indicating that temperature is having little effect on the oxidation of the Ni {111} surface.

VI. SURFACE PREMELTING

At 2000 K the amount of disorder at the surface layers of the {110} and Ni {111} has become significant. This can be seen from the average atomic coordinates for the

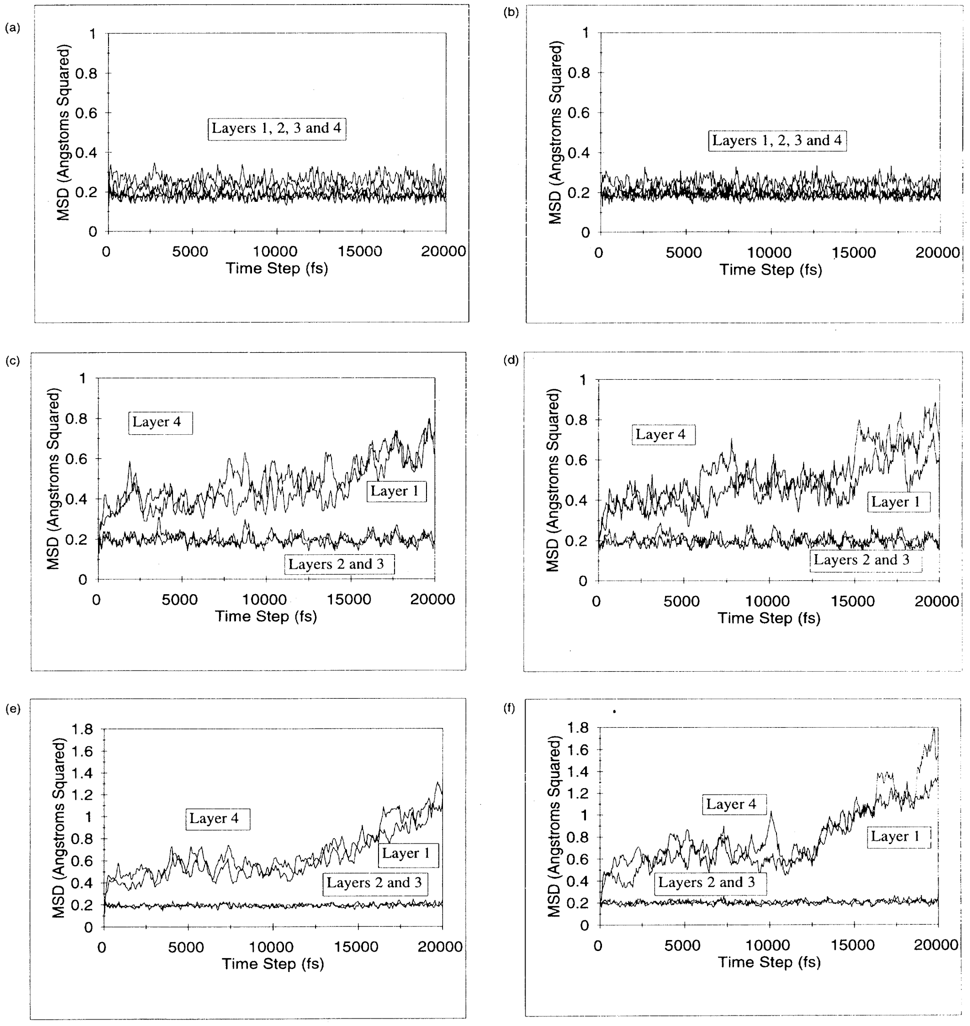

FIG. 8. MSD at 2000 K for Ni^{2+} and O^{2-} as a function of layer for (a) and (b) the {100} surface, (c) and (d) the {110} surface, and (e) and (f) the Ni {111} unoxidized surface.

20-ps data-collecting run and are shown in Figs. 3, 6, and 7 for the {110}, {100}, and Ni {111} surfaces, respectively, at 2000 K. For the {100} surface the average atomic positions correspond closely with the lattice positions of the initial structure. However, at the {110} and Ni {111} surfaces there is considerable disorder, which is most evident for the Ni {111}. The disorder observed could be interpreted as premelting. There are two forms that this could take: surface roughening, or the formation of a quasiliquid layer.[4] If the surface had formed a quasiliquid layer, atomic movement at the surface would be greatly increased.

Atomic transport at the surface can be calculated using the mean-squared displacements (MSD's) of the ions from their original positions. The MSD of an ion is given by the following equation:

$$r_i^2=\frac{1}{N_i}\sum_i[(x_{i(t)}-x_{i(0)})^2+(y_{i(t)}-y_{i(0)})^2+(z_{i(t)}-z_{i(0)})^2] ,$$

where x, y, and z are the ions' coordinates at the start and at time t. If there is no increase in the MSD of an ion type with time, then the ions are vibrating about their mean lattice site. If the MSD's increase with time, then the ions are considered to be moving away from their initial positions.

The surface slabs are divided into equal regions lying perpendicular to the stacking direction and the MSD calculated for each region. The MSD's are given in Fig. 8 for both Ni^{2+} and O^{2-} ions in each of the three surfaces {100}, {110}, and Ni {111}. From these plots it is clear that the ions in the surface layers (layers 1 and 4) of the {110} and Ni {111} surfaces are loosely bound to the surface and are free to move. The MSD's for both Ni^{2+} and O^{2-} in the {110} and stoichiometric Ni {111} surface are similar, indicating that no sublattice diffusion is taking place and the surface is molten. The peak MSD of Ni^{2+} for the {110} of 0.8 Å^2 is less than the stoichiometric Ni {111} surface of 1.3 Å^2 indicating that the ions on the Ni {111} surface have greater freedom of movement.

The ordering of the oxidized Ni {111} surface is reflected in the MSD's of Ni^{2+}, Ni^{3+}, and O^{2-} as a function of depth given in Fig. 9. The degree of ion movement for this oxidized surface is much less than for the stoichiometric Ni {111} surface. The surface Ni^{3+} ions are not moving appreciably, with a peak MSD of 0.36 Å^2 compared to the stoichiometric surface of 1.3 Å^2. The movement of the surface O^{2-} ions is also reduced to 0.9 Å^2 compared to 1.8 Å^2, although this is still larger than the center of the slab with a MSD of 0.2 Å^2. The more densely packed surface of the oxidized Ni {111} surface is therefore inhibiting ion movement along the surface.

Experimentally, premelting has been seen for metals[34] using scanning electron microscopy to observe the equilibrium forms of Bi and Pb crystals below the bulk melting point. Simulations using the embedded-atom method have been performed on the {110} surface of Ni and have indicated surface premelting, forming a quasiliquid layer at about 33 K less than the bulk melting temperature.[35] Simulations by Häkkinen and Manninen[4] on the low index planes of Cu also indicate that surface premelting occurs at approximately 40 K below the melting point of the surface for the {110} Cu surface. The {100} Cu surface stays essentially bulklike and does not premelt. Scanning tunnelling microscopy on the {100}, {110}, and {111} surfaces of Pb indicated that the close-packed surfaces remained intact, while those less densely packed premelted at a significantly lower temperature than the bulk.[36] This agrees well with the results for the molecular-dynamic simulations of the surfaces of NiO

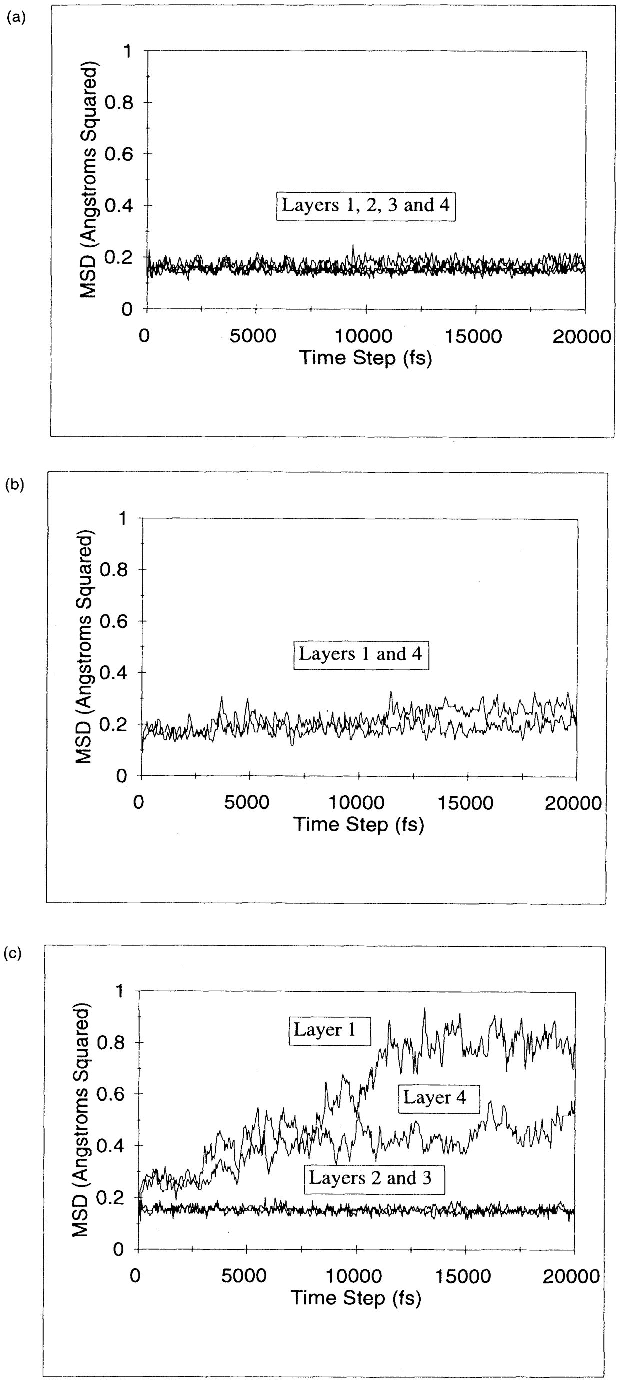

FIG. 9. MSD at 2000 K for (a) Ni^{2+}, (b) Ni^{3+}, and (c) O^{2-} as a function of layer for the oxidized Ni {111} surface.

where the loosely packed surface, the {111}, showed evidence of surface premelting, while the dense {100} surface shows no premelting.

VII. CONCLUSIONS

The surface energies for the {100}, {110}, and Ni {111} surfaces were calculated as a function of temperature using molecular dynamics. The surface energies for the {110} and Ni {111} surfaces decreased with temperature up to 2000 K, whereas the surface energy for the {100} remained essentially constant.

At 2000 K the {110} and Ni {111} surfaces were disordered with appreciable amounts of diffusion of both Ni^{2+} and O^{2-} ions at the surface indicating premelting of the surface. The more densely packed {100} surface showed no such behavior. This is in agreement with previous calculations on the {110} Ni and Cu metal surfaces. For the defective Ni^{3+} Ni {111} surface the results indicate that the oxidation energy is similar to the static calculation, the MD simulation being 0.2 eV/Ni^{3+} more favorable. This indicates that the surface will oxidize whenever possible, although the kinetics of this process are not available from this work. The MSD's of the oxidized Ni {111} surface show that there is much less movement of ions at the surface compared to the stoichiometric surface. This could be due to increased charge at the surface, with the resulting reconstruction leading to a densely packed surface layer.

The temperatures at which the crystal melts were 3400, 3000, and 2800 K for the {100}, {110}, and Ni {111} surfaces, respectively. This indicates that the temperature at which a crystal melts is governed by surfaces. The oxidized Ni {111} surface melts at 3000 K, which is higher than the nonoxidized surface, reflecting the more ordered surface structure.

The results indicate that when determining the melting point of a crystal using surface slabs it is very important to consider a variety of surfaces, since the {110} and {111} surfaces of NiO melted before the {100}, which remained bulklike. The thickness of the slabs also has to be considered, because, if only very thin slabs were used, then the present simulations would indicate that NiO melts at 2000 K (using the data for the {111} surface). Thus the use of thin slabs could seriously compromise the simulations, as effects such as surface premelting would be interpreted as crystal melting.

ACKNOWLEDGMENTS

We would like to thank EPSRC, ICI C&P Ltd. for funding, and Biosym Technologies for the provision of Insight II.

---

*Electronic address: P. M. Oliver@bath.ac.uk.
†Electronic address: G. Watson@bath.ac.uk.
‡Electronic address: S. C. Parker@bath.ac.uk.

[1] J. H. Harding, Rep. Prog. Phys. **53**, 1403 (1990).
[2] E. A. Colbourn, Surf. Sci. Rep. **15**, 281 (1992).
[3] C. R. A. Catlow, J. D. Gale, and R. W. Grimes, J. Solid State Chem. **106**, 13 (1993).
[4] H. Häkkinen and M. Manninen, Phys. Rev. B **46**, 1725 (1992).
[5] D. M. Duffy and P. W. Tasker, Philos. Mag. A **54**, 759 (1986).
[6] S. C. Parker, J. O. Titiloye, and G. W. Watson, Philos. Trans. R. Soc. London Ser. A **34**, 37 (1993).
[7] P. Masri and P. W. Tasker, Surf. Sci. **149**, 209 (1985).
[8] S. C. Parker and G. D. Price, Adv. Solid State Chem. **1**, 295 (1989).
[9] R. Ferneyhough, D. Fincham, G. D. Price, and M. J. Gillan, Model. Simul. Mater. Sci. Eng. **2**, 1101 (1994).
[10] C. A. Handwerker, M. D. Vaudin, and J. E. Blendell, J. Phys. (Paris) Colloq. Suppl. 10, **49**, C5367 (1988).
[11] W. E. Ford and E. S. Dana, *A Textbook of Mineralogy,* 4th ed. (Wiley, New York, 1958).
[12] P. M. Oliver, S. C. Parker, and W. C. Mackrodt, Mod. Simul. Mater. Sci. Eng. **1**, 755 (1993).
[13] M. Matsui, J. Chem. Phys. **91**, 489 (1989).
[14] G. W. Watson, S. C. Parker, and A. Wall, J. Phys. Condens. Matter **4**, 2097 (1992).
[15] M. Parrinello and A. Rahman, J. Appl. Phys. **52**, 7182 (1981).
[16] S. Nose, J. Chem. Phys. **81**, 511 (1984).
[17] W. G. Hoover, Phys. Rev. A **31**, 1695 (1985).
[18] P. W. Tasker, J. Phys. C **12**, 4977 (1979).
[19] F. Bertaut, Compt. Rend. **246**, 3447 (1958).
[20] M. J. L. Sangster and A. M. Stoneham, Philos. Mag. B **43**, 597 (1981).
[21] M. J. Gillan, Physica **131B**, 157 (1985).
[22] P. W. Tasker and D. M. Duffy, Surf. Sci. **137**, 91 (1984).
[23] W. Reichardt, V. Wagner, and W. Kress, J. Phys. C **8**, 3995 (1975).
[24] P. J. Gielisse, J. N. Plendl, L. C. Mansur, R. Marshall, S. S. Mitra, R. Mykolajewycz, and A. Smakula, J. Appl. Phys. **36**, 2446 (1965).
[25] *Numerical Data and Functional Relationships in Science and Technology,* edited by K. H. Hellwege, Landolt-Börnstein, New Series, Group III, Vol. 11 (Springer-Verlag, Berlin, 1979).
[26] R. W. G. Wyckoff, *Crystal Structures* (Wiley, New York, 1963), Vol. 1.
[27] P. J. Mitchell and D. Fincham, J. Phys. Condens. Matter **5**, 1031 (1993).
[28] P. J. D. Lindman and M. J. Gillan, J. Phys. Condens. Matter **5**, 1019 (1993).
[29] D. Fincham, W. C. Mackrodt, and P. J. Mitchell, J. Phys. Condens. Matter **6**, 393 (1994).
[30] C. Massobrio and M. Meyer, J. Phys. Condens. Matter **3**, 279 (1991).
[31] N. H. de Leeuw, S. C. Parker, and G. W. Watson, J. Phys. Chem. (to be published).
[32] P. M. Oliver, S. C. Parker, J. Purton, and D. W. Bullett, Surf. Sci. **307-309**, 1200 (1994).
[33] M. Gajdardziska-Josifovska, P. A. Crozier, and M. R. McCartney, Surf. Sci. **284**, 186 (1993).
[34] A. Pavlovska, D. Dobrev, and E. Bauer, Surf. Sci. **286**, 176 (1993).
[35] E. T. Chen, R. N. Barnett, and Uzi Landman, Phys. Rev. B **41**, 439 (1990).
[36] J. W. M. Frenken, H. M. van Pinxteren, and L. Kuipers, Surf. Sci. **283**, 283 (1993).

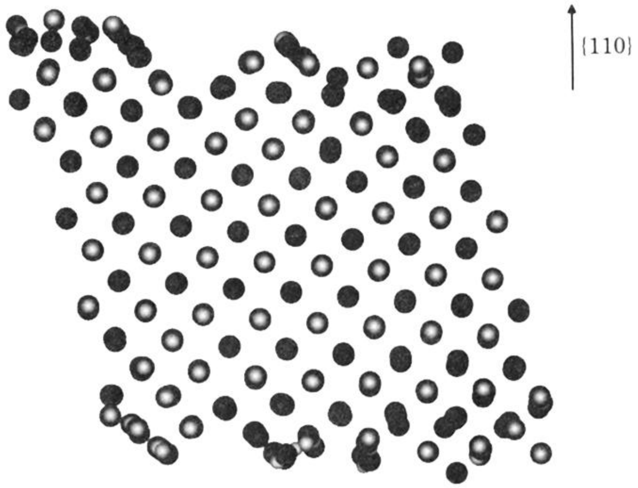

FIG. 3. Average coordinate positions at 2000 K for the {110} surface of NiO [Ni^{2+} (gray) and O^{2-} (black)].

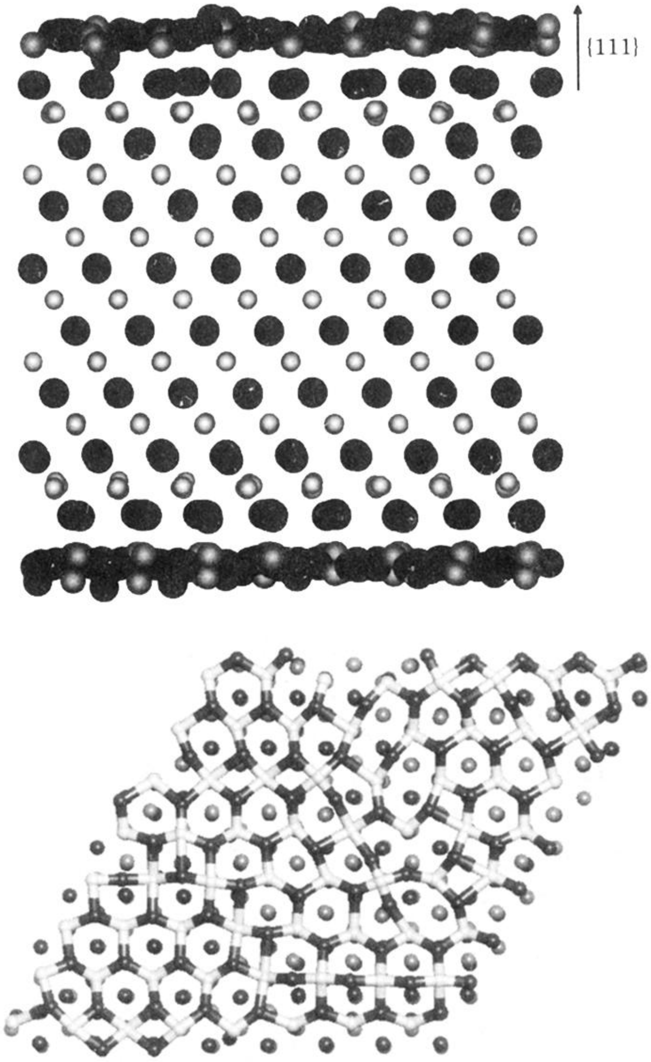

FIG. 5. Average coordinate positions at 2000 K for the oxidized Ni {111} surface showing (a) side view and (b) plan view with surface order emphasized with tubular bonds [Ni^{2+} (gray), Ni^{3+} (large gray), and O^{2-} (black)].

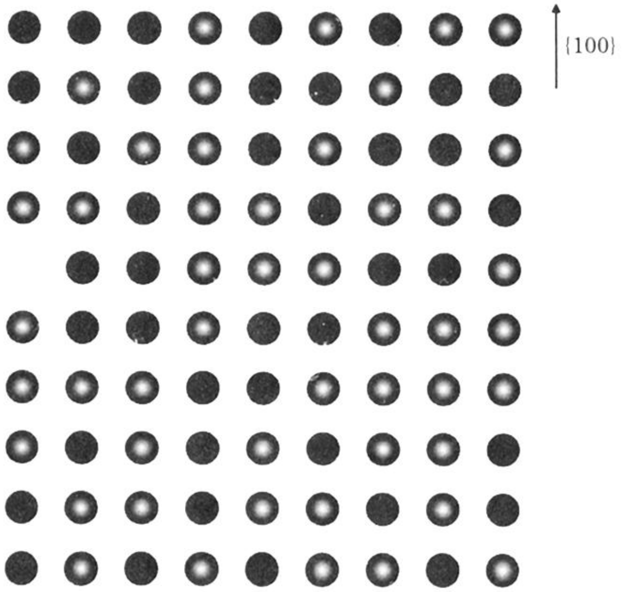

FIG. 6. Average coordinate positions at 2000 K for the {100} surface of NiO [Ni^{2+} (gray) and O^{2-} (black)].

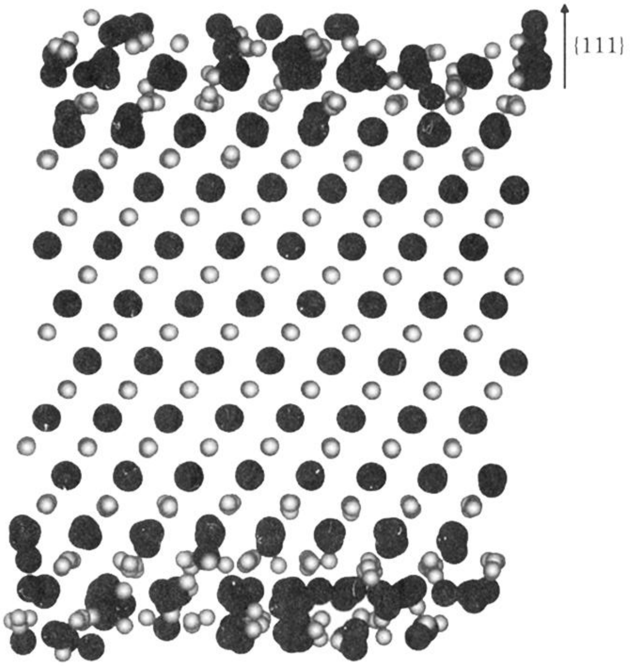

FIG. 7. Average coordinate positions at 2000 K for the Ni {111} surface of NiO [Ni^{2+} (gray) and O^{2-} (black)].